Appendix A.54:

455 Papanui Rd – VsVp 57189

Table 1: Site Description for 455 Papanui Road (VsVp 57189).

Attribute	Yes/No			Description/Date	Symbol in Figure 1
	10-m Buffer	20-m Buffer	50-m Buffer		
Near a body of surface water or other free face features?	No	No	No	The center of the site is ~50 m to the NE from unnamed stream (the free-face height is ~0.5 m).	NA
Lateral spreading observed during the CES?	No	No	No	No lateral spreading was observed by the mapping team.[1]	NA
Nearby buildings or structures?	No	Yes	Yes	Building coverage of the 20-m and 50-m buffers is 8% and 13%, respectively.	NA
Sloping land?	No	No	No	Flat land, open field +residential area	NA
Step changes in the ground surface?	No	No	No	NA	NA
Retaining walls?	No	No	No	NA	NA
Vegetation?	No	No	Yes	Trees and bushes cover 10% of the 50-m buffer. They are in all quadrants of the 50-m buffer.	NA
Anthropogenic changes to the site between the LiDAR surveys?	ND	ND	ND	Not evaluated because LiDAR surveys were not used to estimate the ejecta-induced settlement at the site. Ejecta were evidently absent from the site.	NA
Other important factors?	No	No	Yes	Moderate-motor-vehicle-volume roads (Papanui Rd and Blighs Rd) cover 27% of the 50-m buffer; they occupy the NE, SE and SW quadrants of the 50-m buffer.	NA

Note: Buffer is the area within a circle of a specified radius with VsVp investigations done at its center (172.610136°, -43.499954°).

[1] Canterbury Geotechnical Database. (2012). "Observed Ground Crack Locations", Map Layer CGD0400 - 23 July 2012, retrieved July 09, 2018 from https://canterburygeotechnicaldatabase.projectorbit.com/

Figure 1: Site plan.

Note 1: The LiDAR surveys were not considered for the ejecta-induced settlement assessment because the site had no ejecta.

Table 2: LiDAR flight error adjustments, global adjustments for the difference between average LiDAR point elevations and benchmark survey elevations, and vertical tectonic movement adjustments.

	Adjustments (mm)		
Earthquake Event(s)	LiDAR Flight Error	Global Offset[2]	Tectonic Vertical Movement
Sep-10	0	-3	0
Feb-11	0	16	-45
Jun-11	0	38	-25
Dec-11	-50	-65	0
CES	-50	-14	-70
Any LiDAR survey affected by ejecta?			No

Note: The negative sign indicates the subtraction from the ground surface subsidence, while the positive sign indicates the addition to the ground surface subsidence.

[2] Russell, J., & van Ballegooy, S. (2015). *Canterbury Earthquake Sequence: Increased liquefaction vulnerability assessment methodology*. New Zealand: Tonkin & Taylor Ltd.

Table 3: Ejecta-Induced settlement for the top 20 m of the soil profile for the 50th %ile PGA, P_L=50%, and C_{FC}=0.13 using BI-2014, ZRB-2002, and I_C cutoff of 2.6.

Earthquake Event(s)	M_W	PGA (g)	Depth to Groundwater (m)	*S_{V1D} (mm)		
				10-m buffer	20-m buffer	50-m buffer
Sep-10	7.1	0.21	1.2	82±20	83±20	85±20
Feb-11	6.2	0.27	1.2	93±50	96±50	97±50
Jun-11	6.2	0.15	1.0	18±25	18±25	21±25
Dec-11	6.1	0.17	1.0	30±50	30±50	36±50

Notes: S_{V1D} = Average vertical settlement due to volumetric compression using Boulanger and Idriss (2014) (BI-2014), Zhang et al. (2002) (ZRB-2002) procedures and de Greef and Lengkeek (2018) thin-layer correction; * indicates that S_{V1D} was calculated to a depth of ~12 m (the maximum CPT depth available due to tip refusal).

Note 2: The uncertainty for volumetric settlement was derived based on the sensitivity of volumetric settlement to PGA, C_{FC}, and P_L for each earthquake event for VsVp 57203 *Shirley Intermediate School* and CC LIQ 1 – CPT 5586 – *Vivian St* sites. Taking the 50th percentile as the baseline case, the minimum and maximum values corresponding to the difference between the 25th percentile and the 50th percentile and the 75th percentile and the 50th percentile were determined. The arithmetic mean of the range of the minimum and maximum difference was evaluated for each patch at the two sites. The maximum arithmetic mean for each earthquake event was rounded to the nearest five and used as the uncertainty value. Accordingly, the 1-D volumetric settlement uncertainties of ±20, ±50, ±25, and ±50 mm for the Sep-10, Feb-11, Jun-11, and Dec-11 earthquake events, respectively, were used for all sites in this study.

Table 4: Best final estimates of ejecta-induced settlement for the site.

EQ Event	10-m buffer			20-m buffer			50-m buffer		
	$S_{E,L}$ (mm)	$S_{E,P}$ (mm)	$S_{E,final}$ (mm)	$S_{E,L}$ (mm)	$S_{E,P}$ (mm)	$S_{E,final}$ (mm)	$S_{E,L}$ (mm)	$S_{E,P}$ (mm)	$S_{E,final}$ (mm)
Sep-10	ND	0	0	ND	0	0	ND	0	0
Feb-11	ND	0	0	ND	0	0	ND	0	0
Jun-11	ND	0	0	ND	0	0	ND	0	0
Dec-11	ND	0	0	ND	0	0	ND	0	0

Notes: $S_{E,L}$ = Ejecta-induced settlement based on LiDAR data was not determined (ND) due to the evident absence of ejecta at the site; $S_{E,P}$ = Ejecta-induced settlement based on ground and aerial photographs and LDAT property inspection reports; $S_{E,final}$ = Best final estimate of ejecta-induced settlement.

Note 3:

- $S_{E,final}$ for all buffers is based solely on $S_{E,P}$ for all earthquake events due to the evident absence of ejecta.
- The 455 Papanui Road site is in the zone of moderate to severe LPI overprediction of liquefaction severity for the Sep-10 EQ and slight to moderate LPI overprediction of

liquefaction severity for the Feb-11 EQ (Maurer et al. 2014[3]). No liquefaction ejecta-induced damage was reported for the properties within the 50-m buffer.

<u>Summary</u>:

The best estimate of the ejecta-induced free-field ground settlement at the 455 Papanui Road site for the SEP 2010, FEB 2011, JUN 2011, and DEC 2011 earthquake is 0 mm, 0 mm, 0 mm, and 0 mm, respectively.

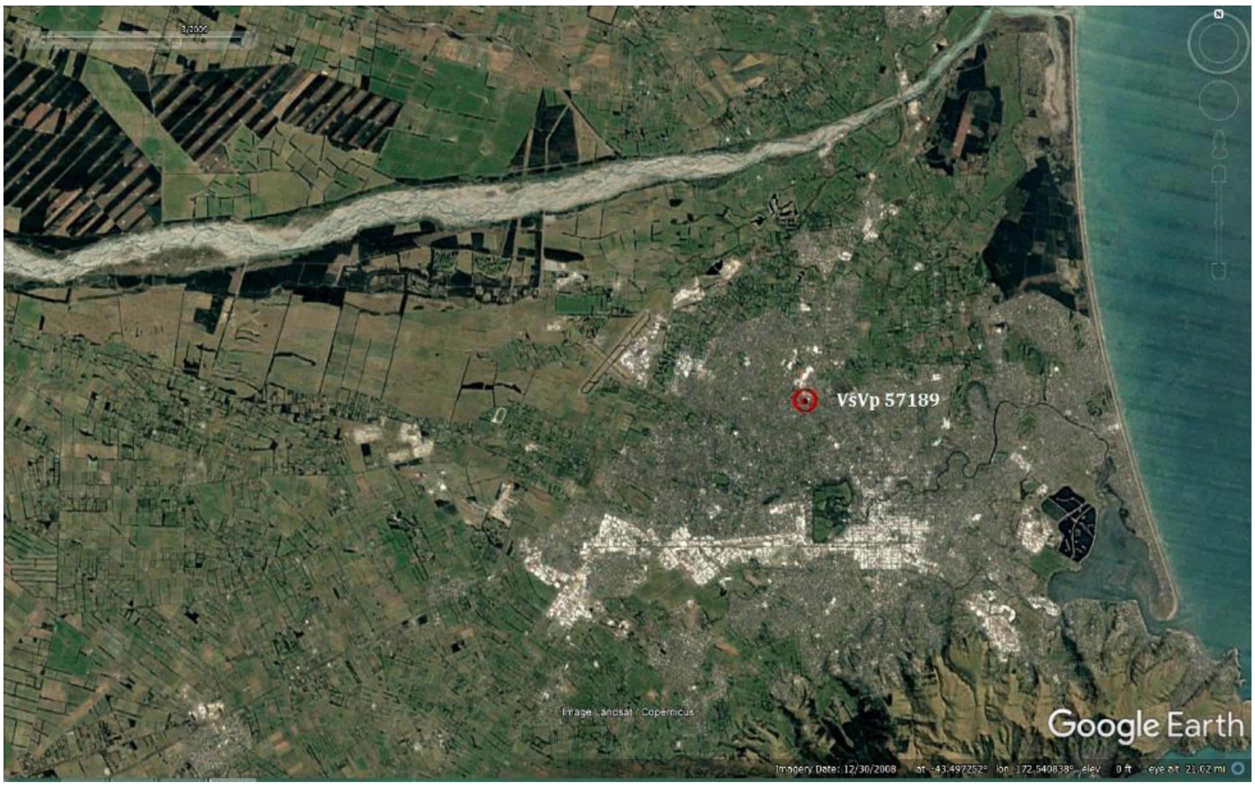

Figure 2: Location of the site.

[3] Maurer, B. W., Green, R. A., Cubrinovski, M., & Bradley, B. A. (2014). Evaluation of the Liquefaction Potential Index for Assessing Liquefaction Hazard in Christchurch, New Zealand. *Journal of Geotechnical and Geoenvironmental Engineering*, 140(7), 04014032-1-11. doi:10.1061/(asce)gt.1943-5606.0001117

Figure 3: Position of the site relative to nearby buildings, vegetation, and free-face features.

Figure 4: Street view of the flat land.

Figure 5: Satellite image of the site taken in Dec 2004.

Figure 6: Satellite image of the site taken in Mar 2009.

Figure 7: Satellite image of the site taken on Sep 3, 2010.

Figure 8: Satellite image of the site taken on Sep 5, 2010.

Figure 9: Satellite image of the site taken on Feb 7, 2011.

Figure 10: Satellite image of the site taken on Feb 23, 2011.

Figure 11: Satellite image of the site taken on Feb 26, 2011.

Figure 12: Satellite image of the site taken on Mar 28, 2011.

Figure 13: Satellite image of the site taken in Apr 2012.

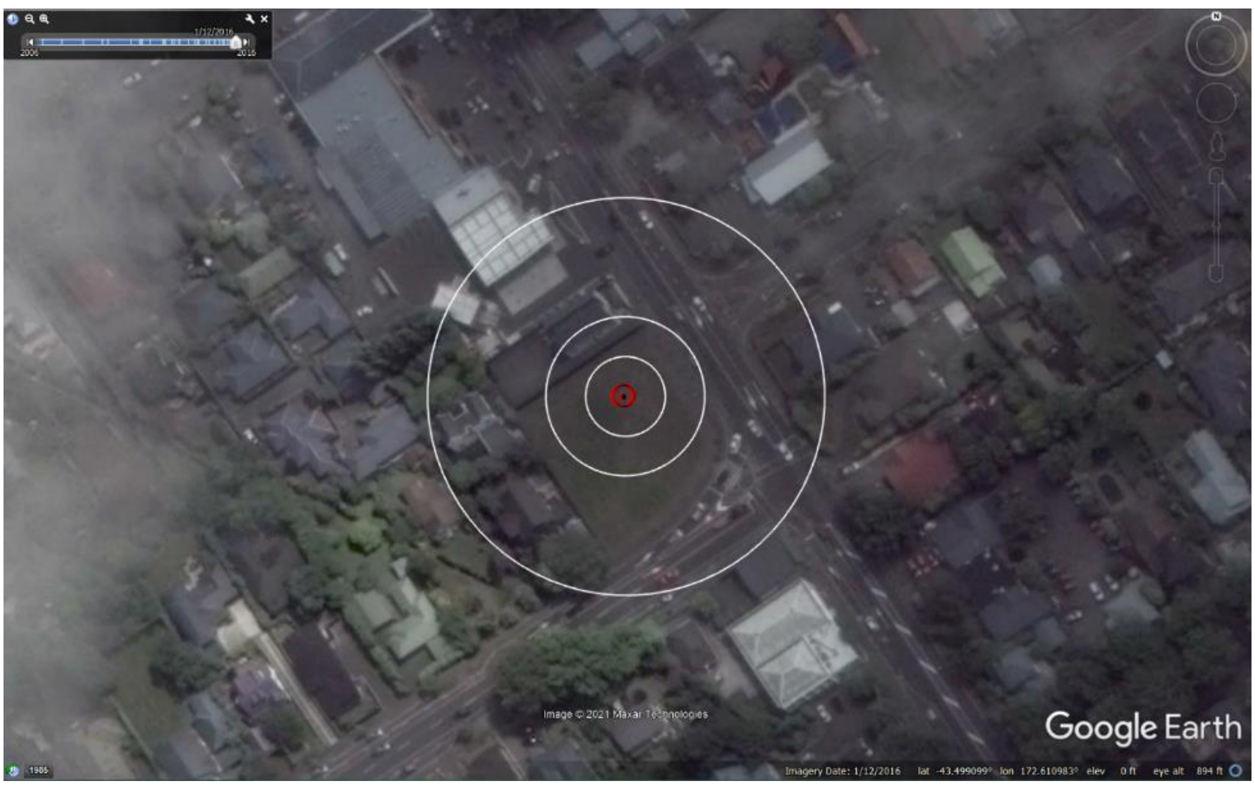

Figure 14: Satellite image of the site taken in Jan 2016.

Figure 15: Aerial photograph of the site taken on Sep 4, 2010.

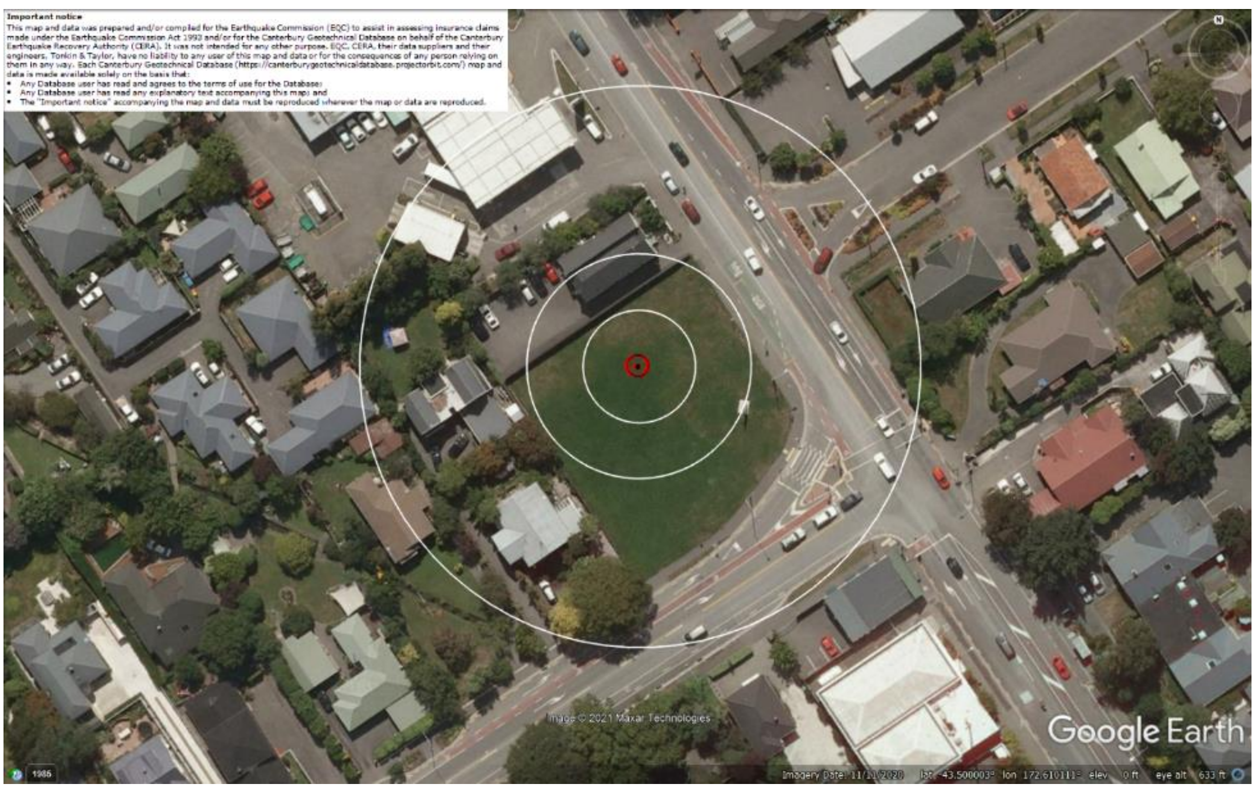

Figure 16: Aerial photograph of the site taken on Feb 24, 2011.

Figure 17: Aerial photograph of the site taken on June 14-15, 2011.

Figure 18: Aerial photograph from June 16, 2011, is not available.

Figure 19: Aerial photograph of the site taken on Dec 24, 2011.

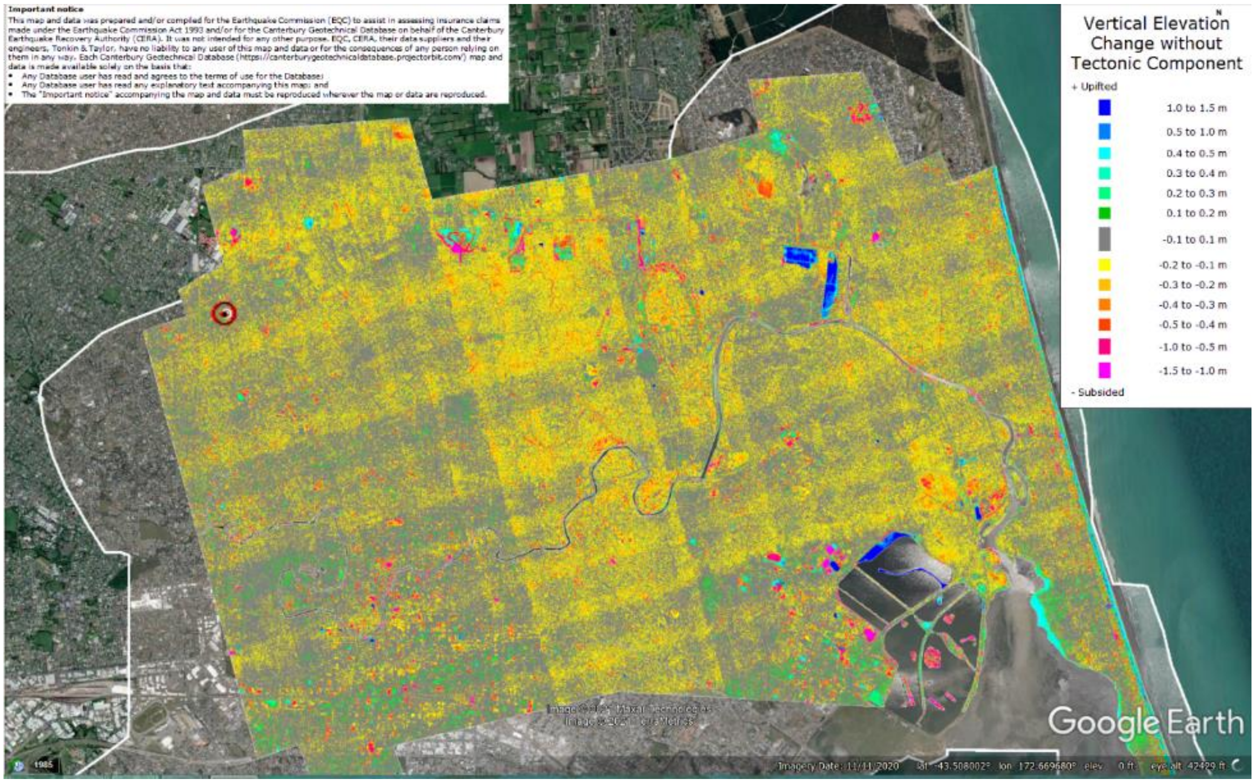

Figure 20: Vertical Ground Movements (Surface – Tectonic) for Sep 2010 Earthquake – the site is not in the apparent zone of overestimated ground surface subsidence.

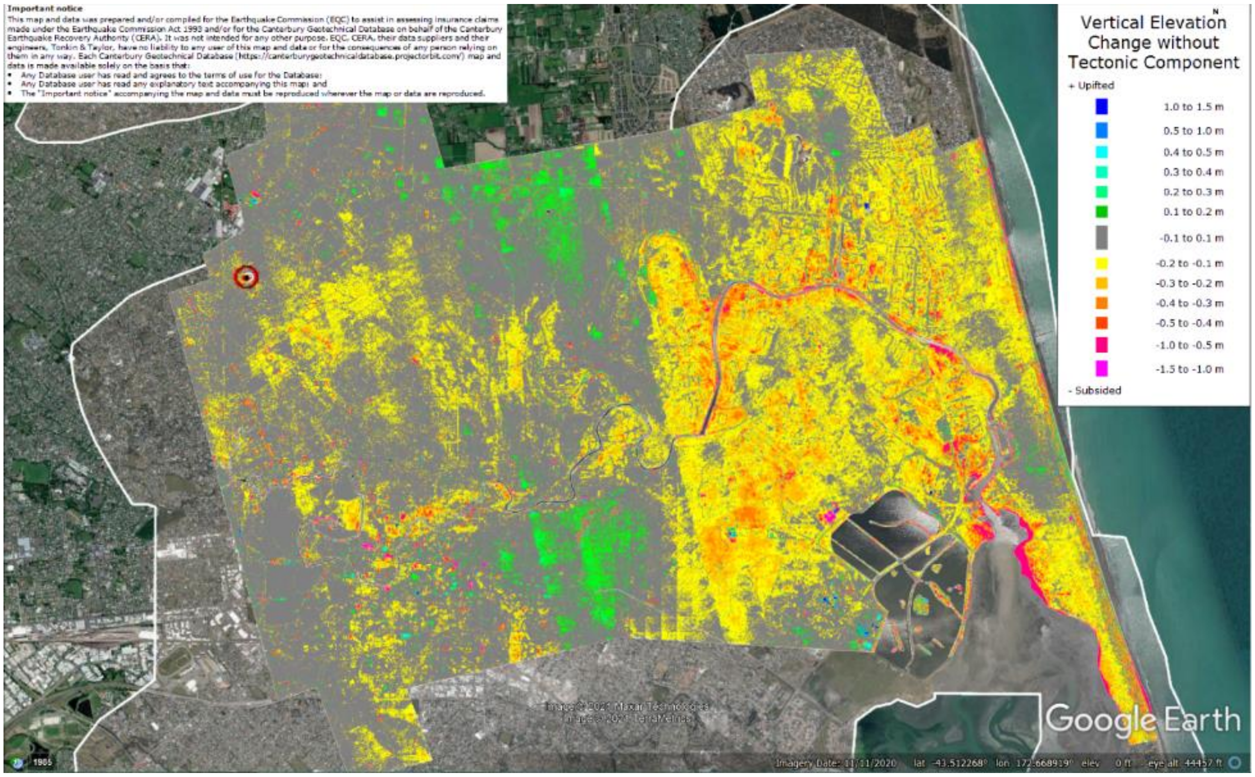

Figure 21: Vertical Ground Movements (Surface – Tectonic) for Feb 2011 Earthquake – the site is not in the apparent zone of underestimated ground surface subsidence.

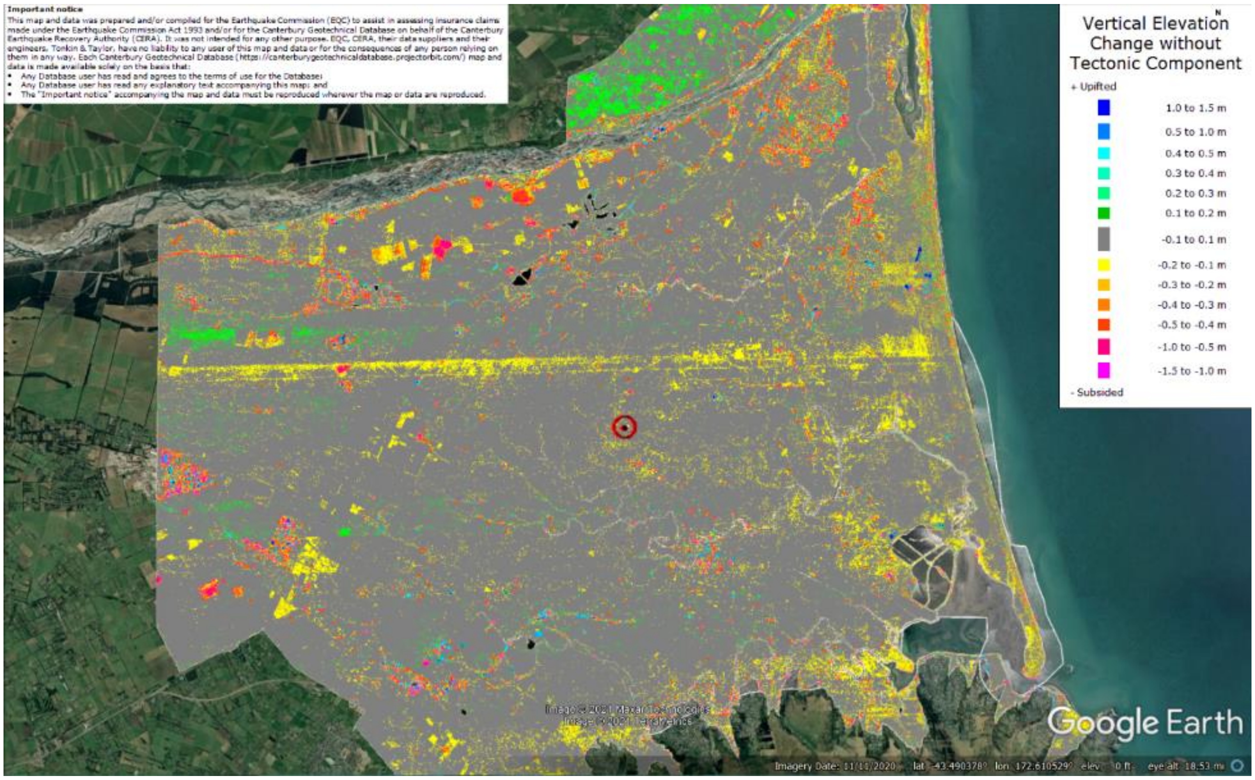

Figure 22: Vertical Ground Movements (Surface – Tectonic) for June 2011 Earthquake – the site is not in the apparent zone of overestimated ground surface subsidence.

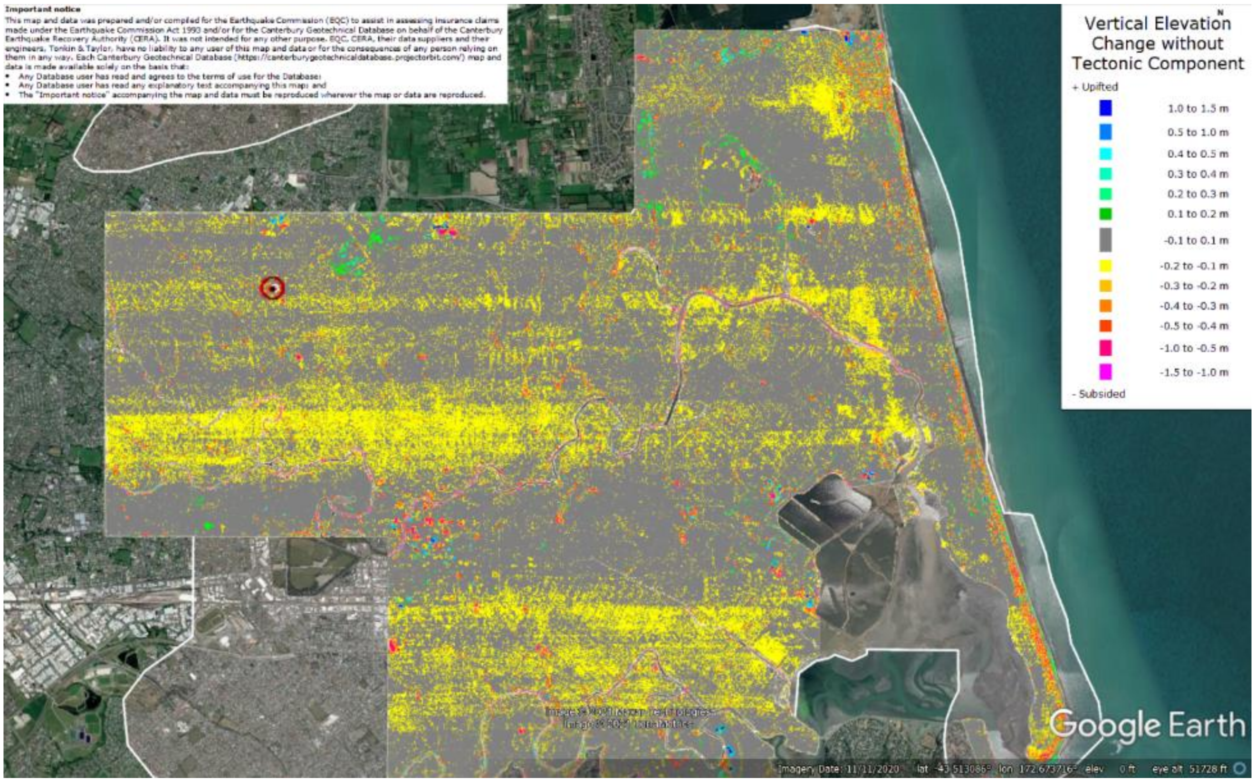

Figure 23: Vertical Ground Movements (Surface – Tectonic) for Dec 2011 Earthquake – the site is in the apparent zone of overestimated ground surface subsidence (i.e., the Feb 2012 LiDAR flight error).

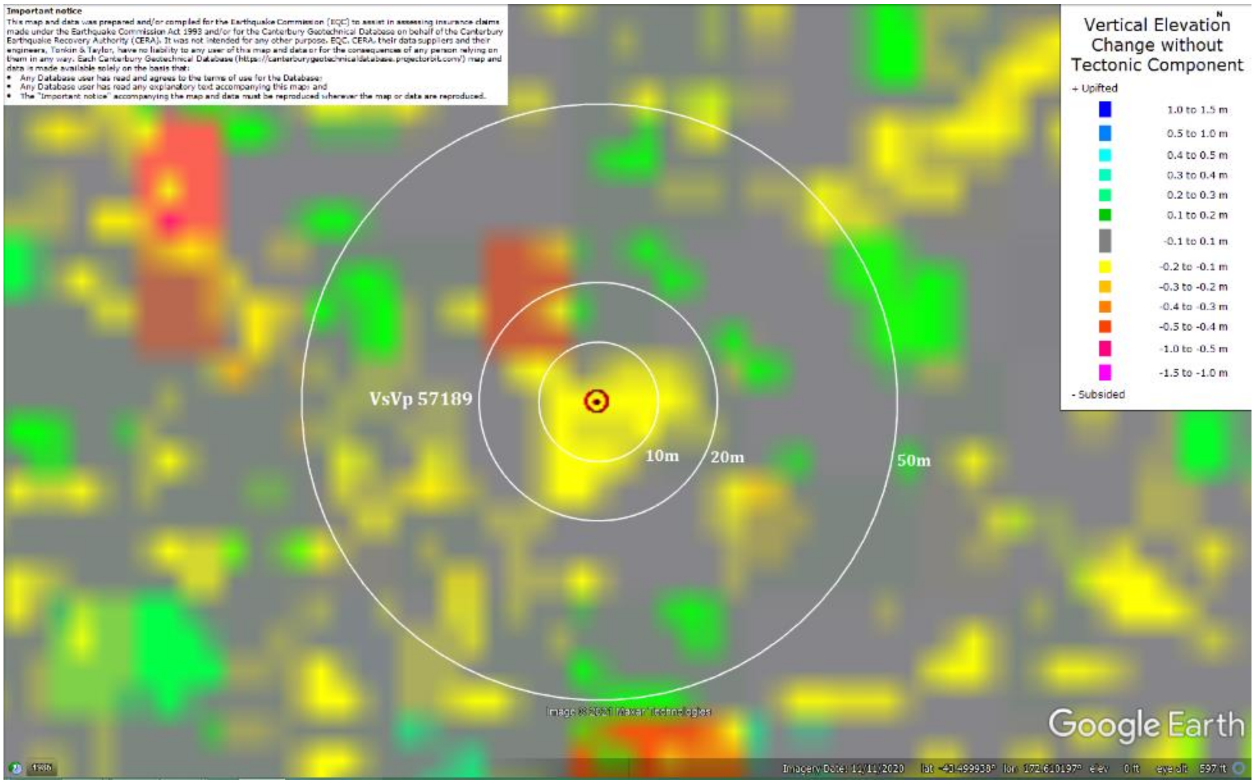

Figure 24: Ground surface subsidence without tectonic component for Sep 2010 Earthquake according to the LiDAR DEM.

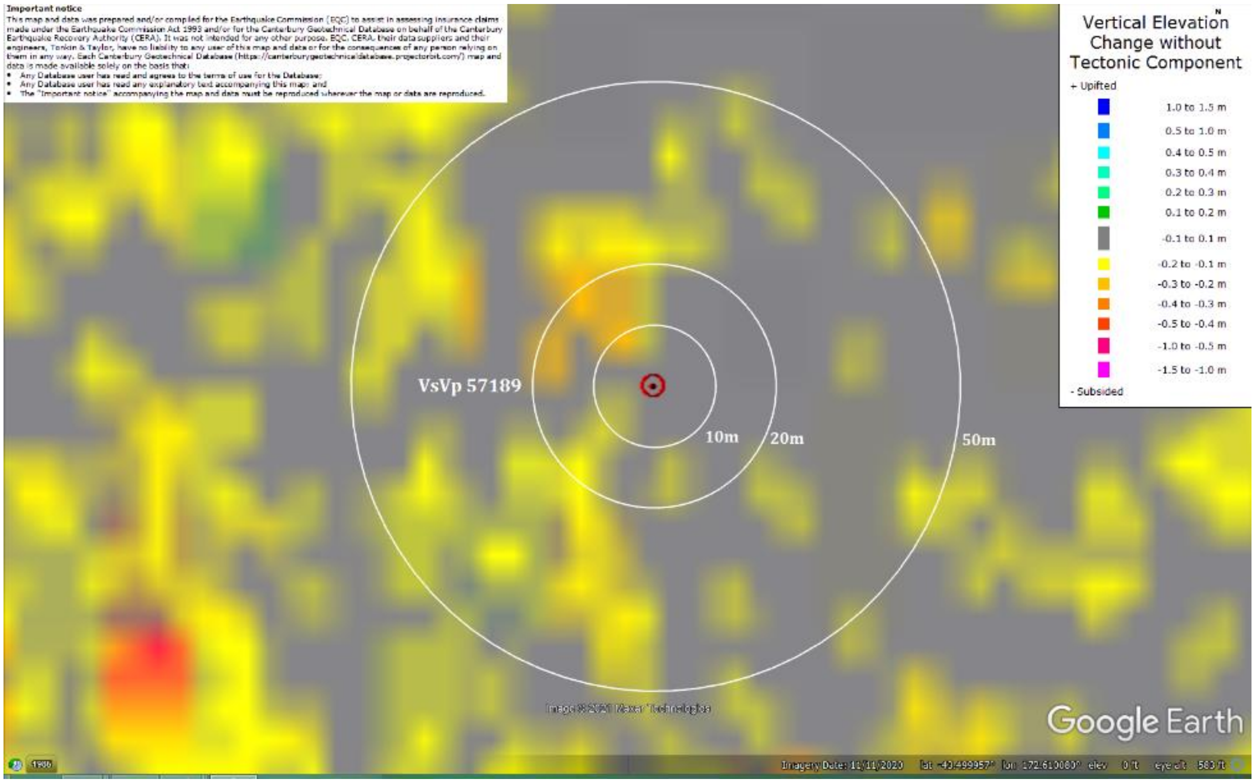

Figure 25: Ground surface subsidence without tectonic component for Feb 2011 Earthquake according to the LiDAR DEM.

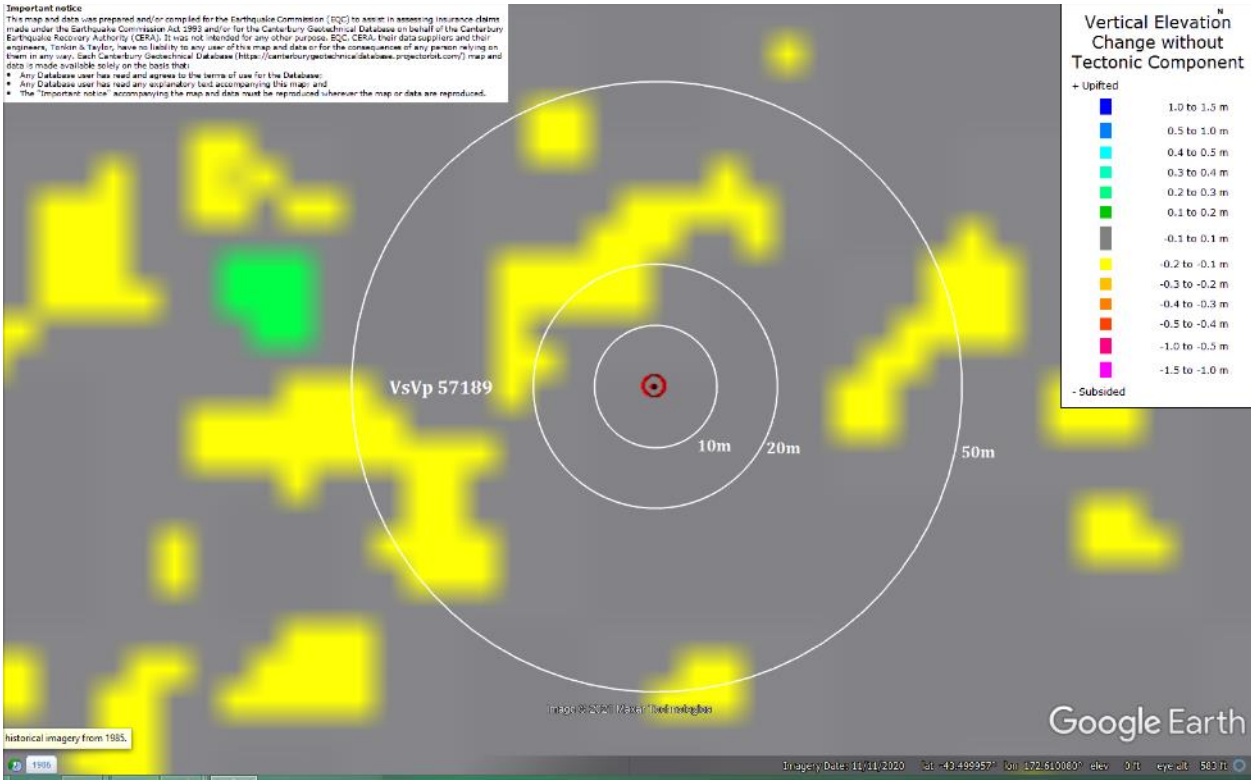

Figure 26: Ground surface subsidence without tectonic component for June 2011 Earthquake according to the LiDAR DEM.

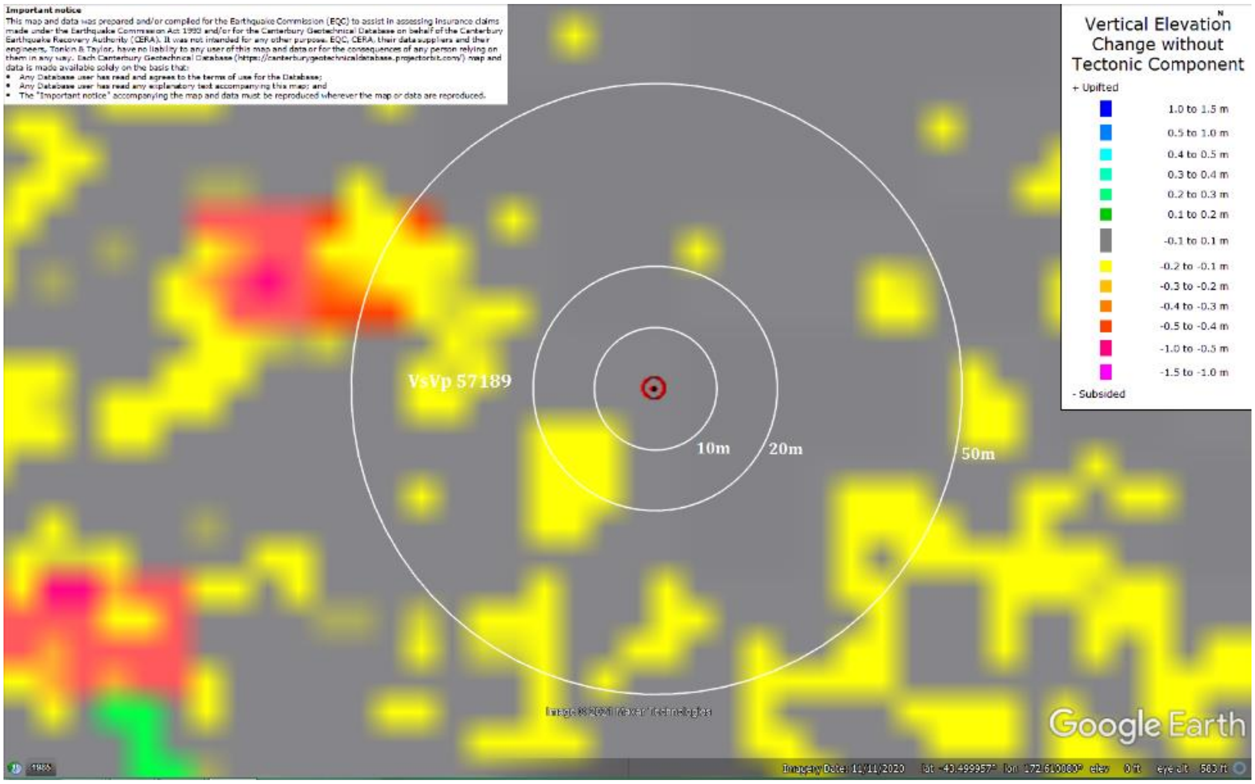

Figure 27: Ground surface subsidence without tectonic component for Dec 2011 Earthquake according to the LiDAR DEM.

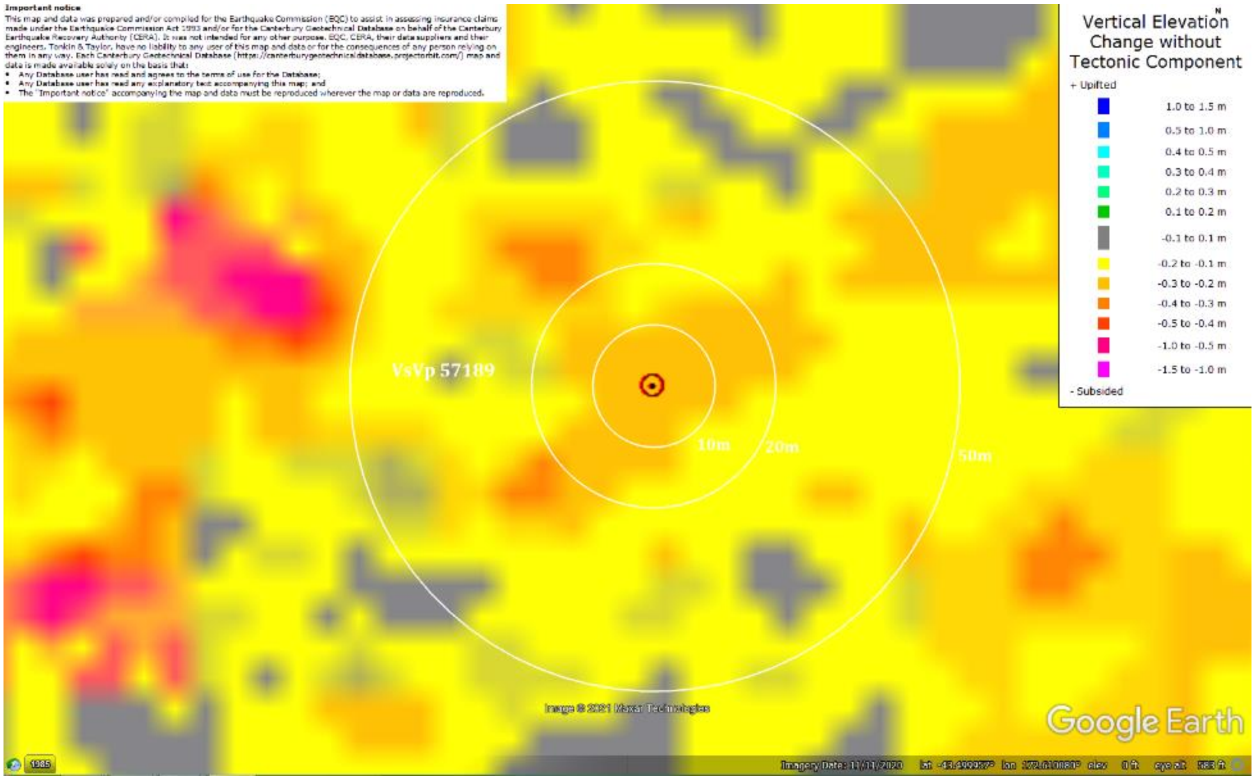

Figure 28: Ground surface subsidence without tectonic component for Canterbury Earthquake Sequence according to the LiDAR DEM.

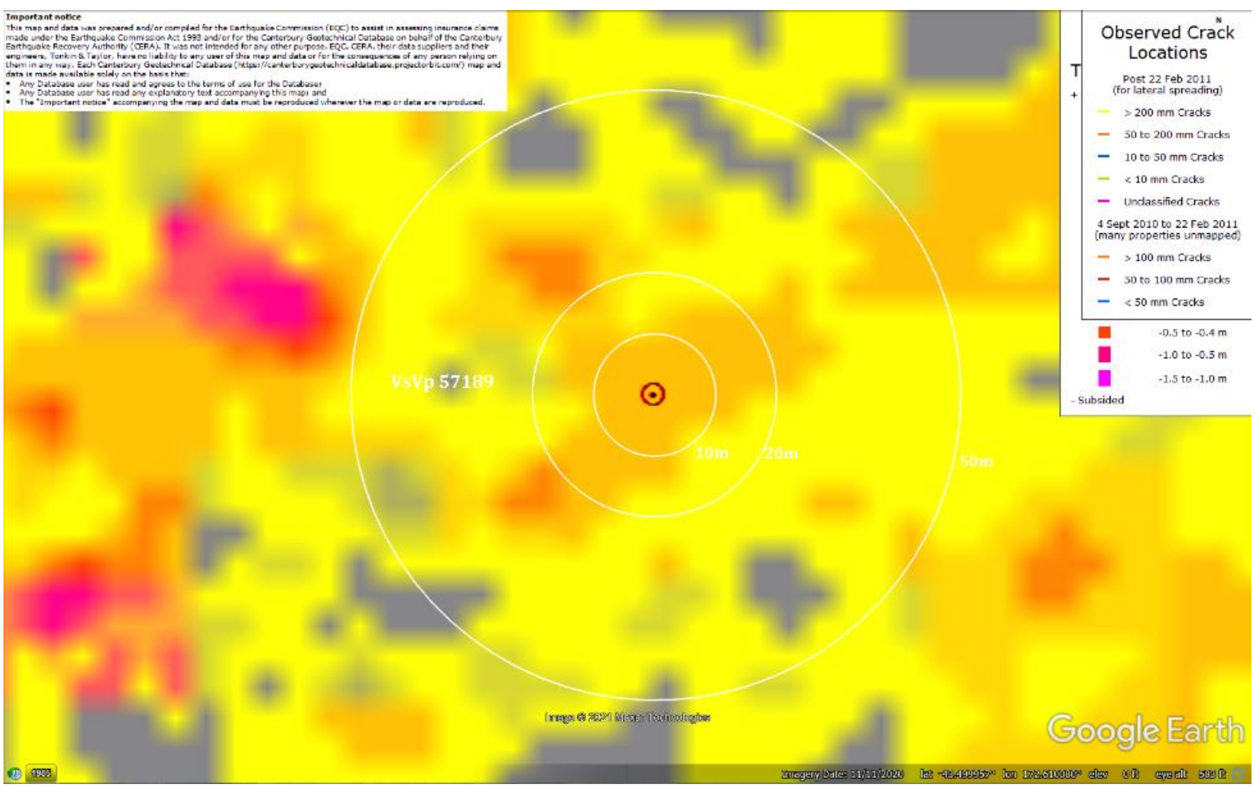

Figure 29: No lateral spreading for Canterbury Earthquake Sequence.

Figure 30: Vertical tectonic movements for Sep 2010 Earthquake.

Figure 31: Vertical tectonic movements for Feb 2011 Earthquake.

Figure 32: Vertical tectonic movements for June 2011 Earthquake.

Figure 33: Vertical tectonic movements for Dec 2011 Earthquake.

Figure 34: Vertical tectonic movements for Canterbury Earthquake Sequence.

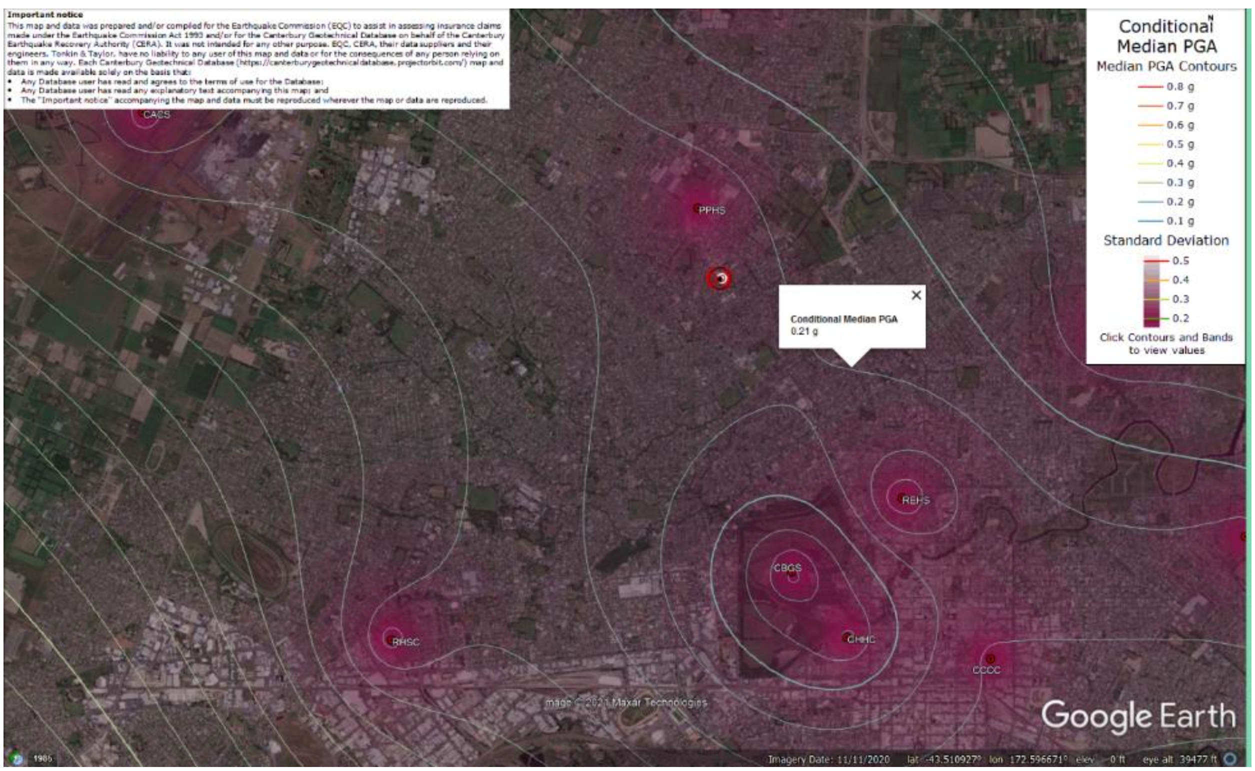

Figure 35: PGA for Sep-10 EQ (st. dev. = 0.275 to 0.300 ln units).

Figure 36: PGA for Feb-11 EQ (st. dev. = 0.300 to 0.325 ln units).

Figure 37: PGA for Jun-11 EQ (st. dev. = 0.325 to 0.350 ln units).

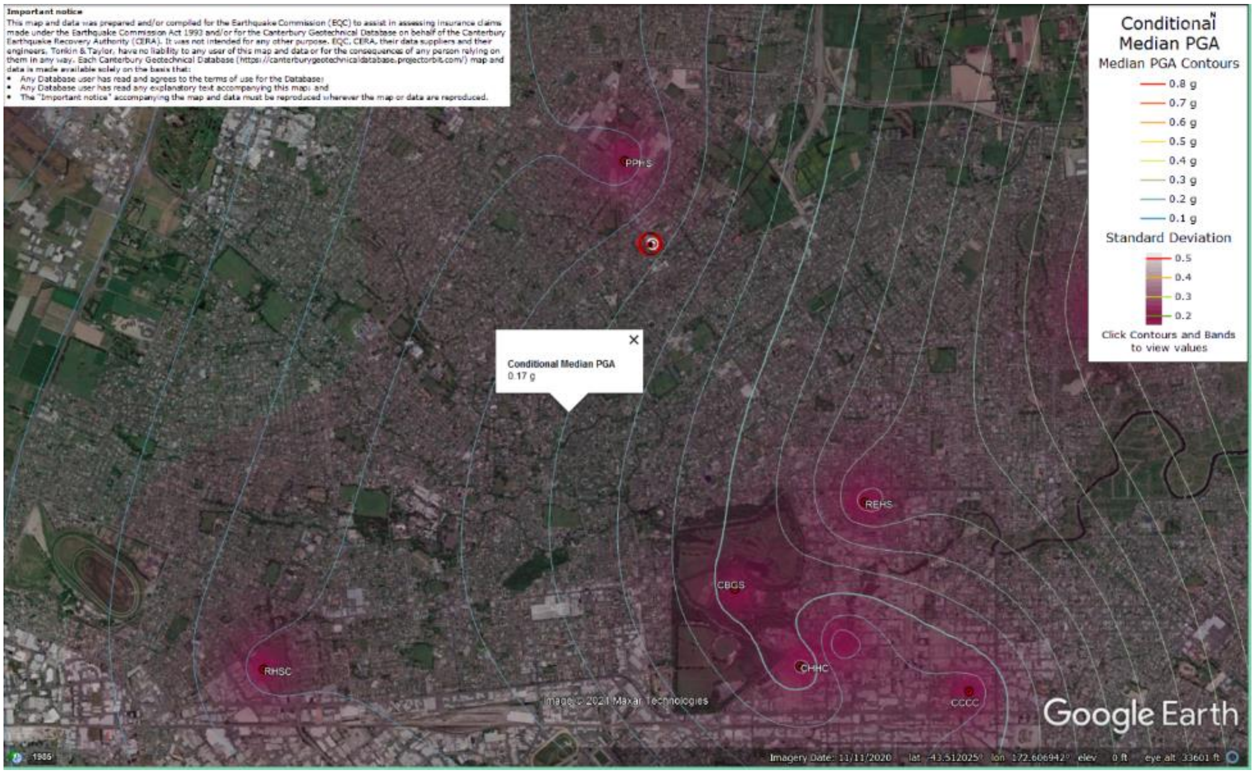

Figure 38: PGA for Dec-11 EQ (st. dev. = 0.325 to 0.350 ln units).

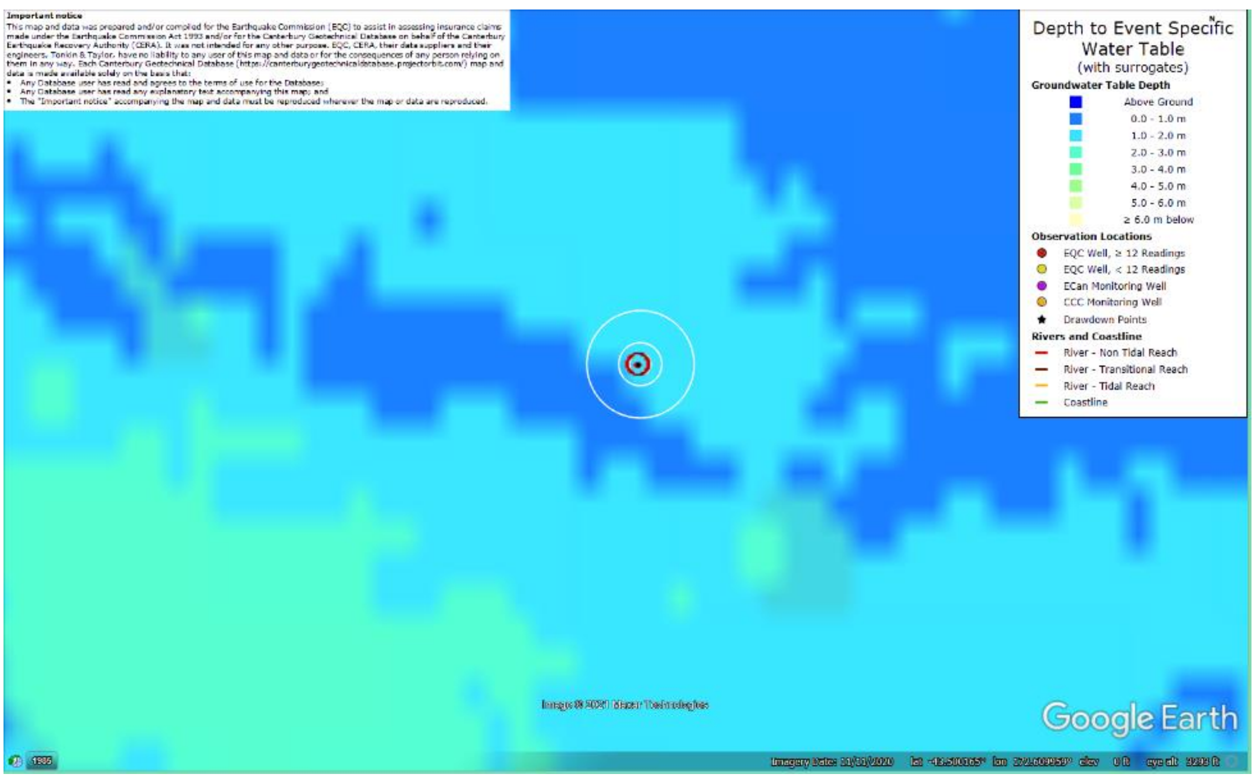

Figure 39: Depth to groundwater table for Sep-10 EQ.

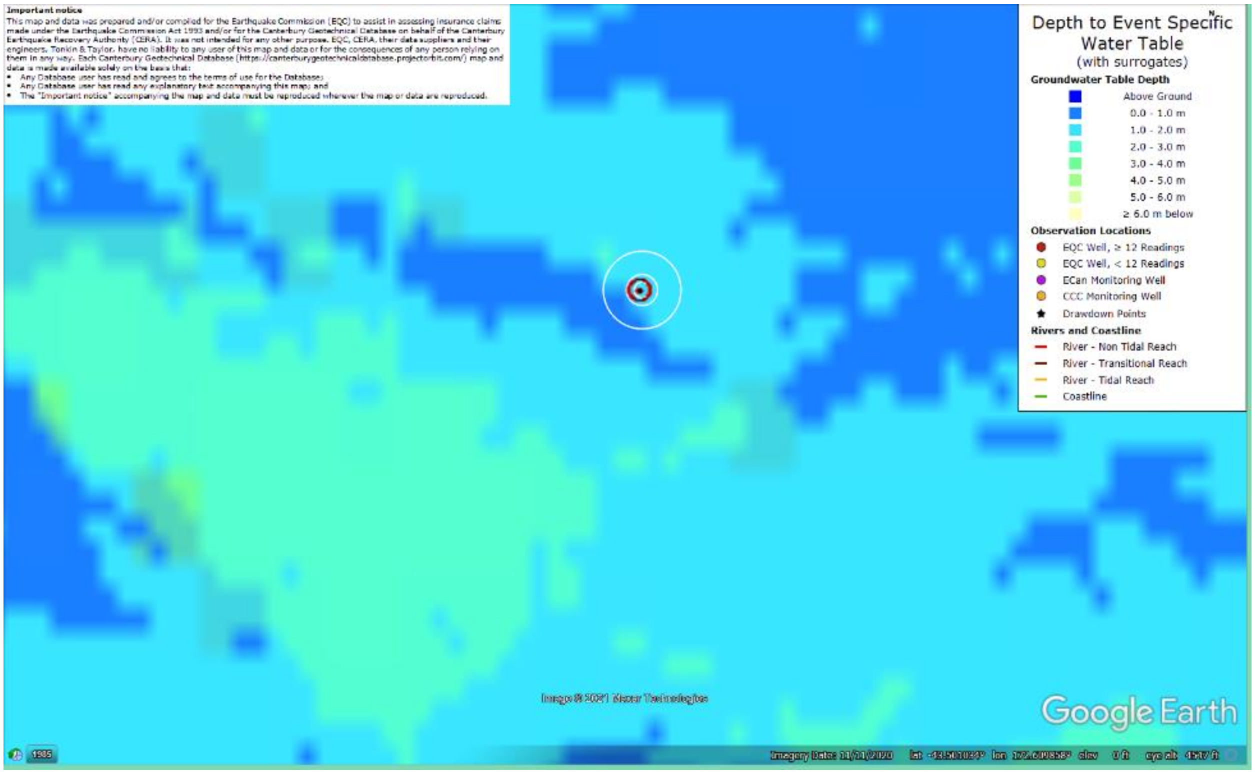

Figure 40: Depth to groundwater table for Feb-11 EQ.

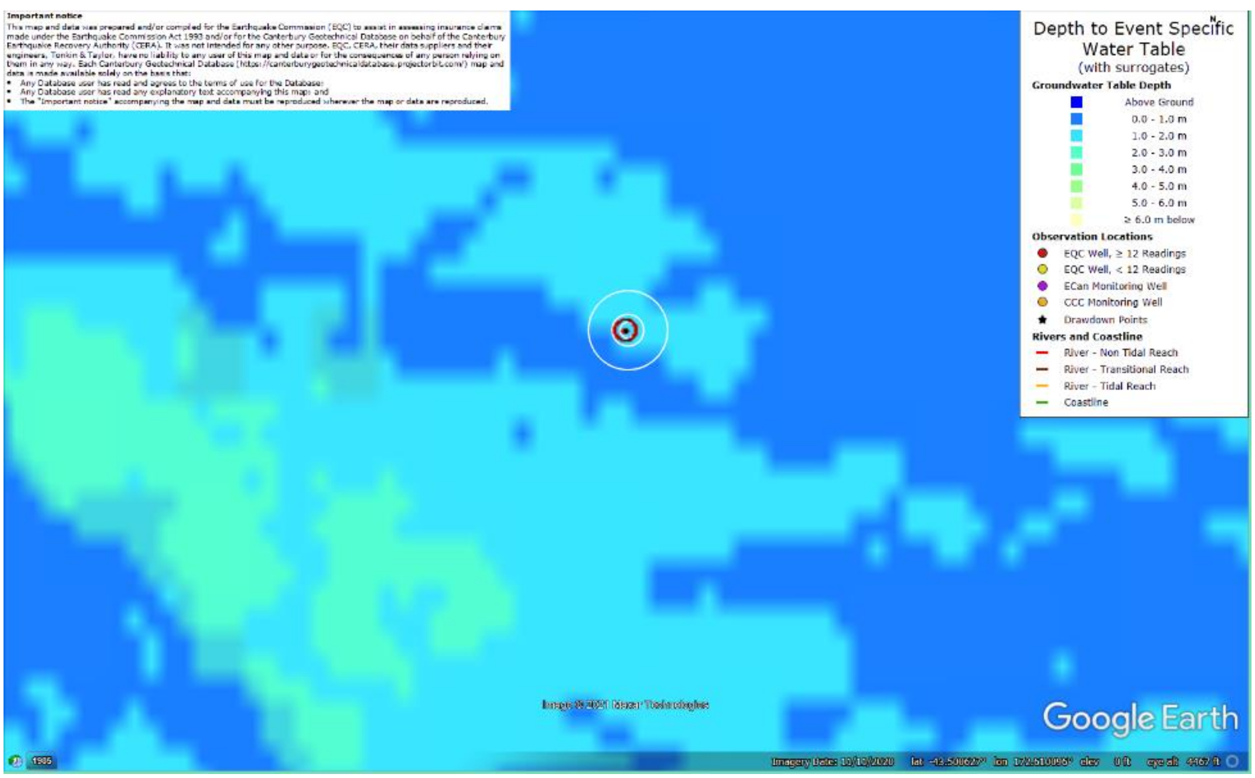

Figure 41: Depth to groundwater table for Jun-11 EQ.

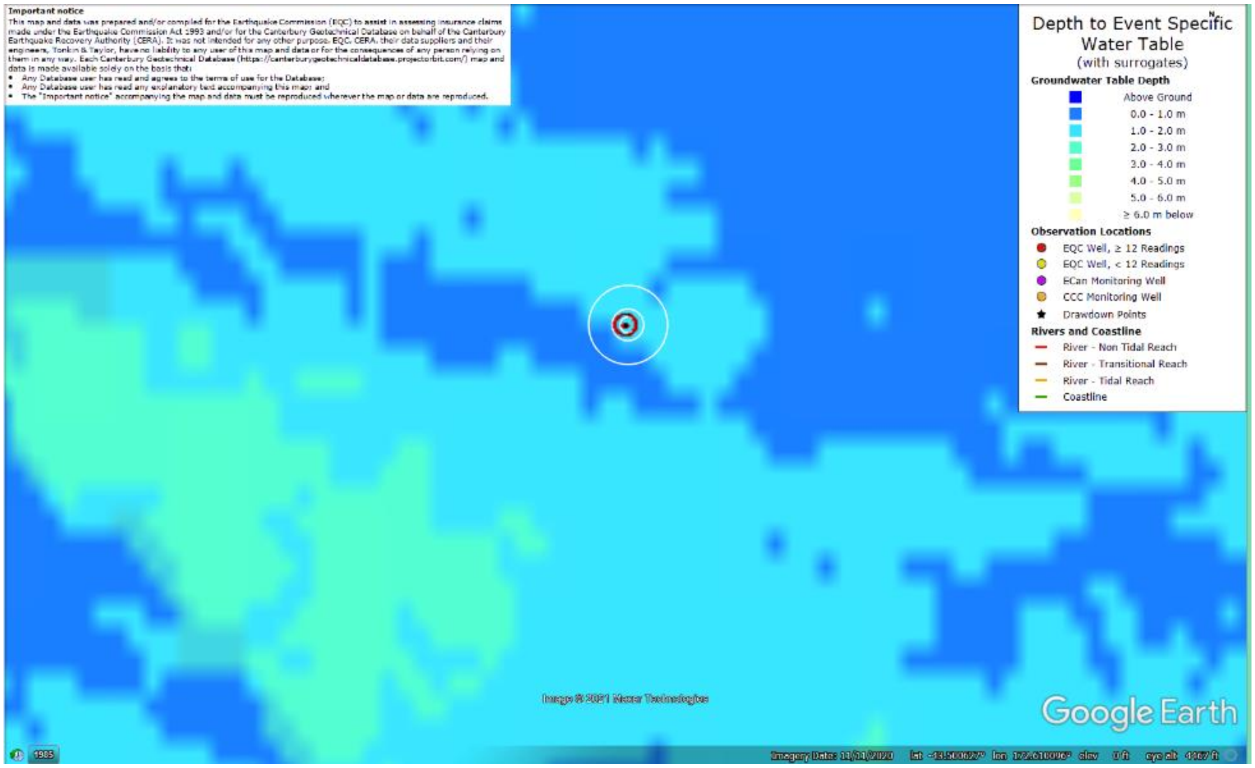

Figure 42: Depth to groundwater table for Dec-11 EQ.

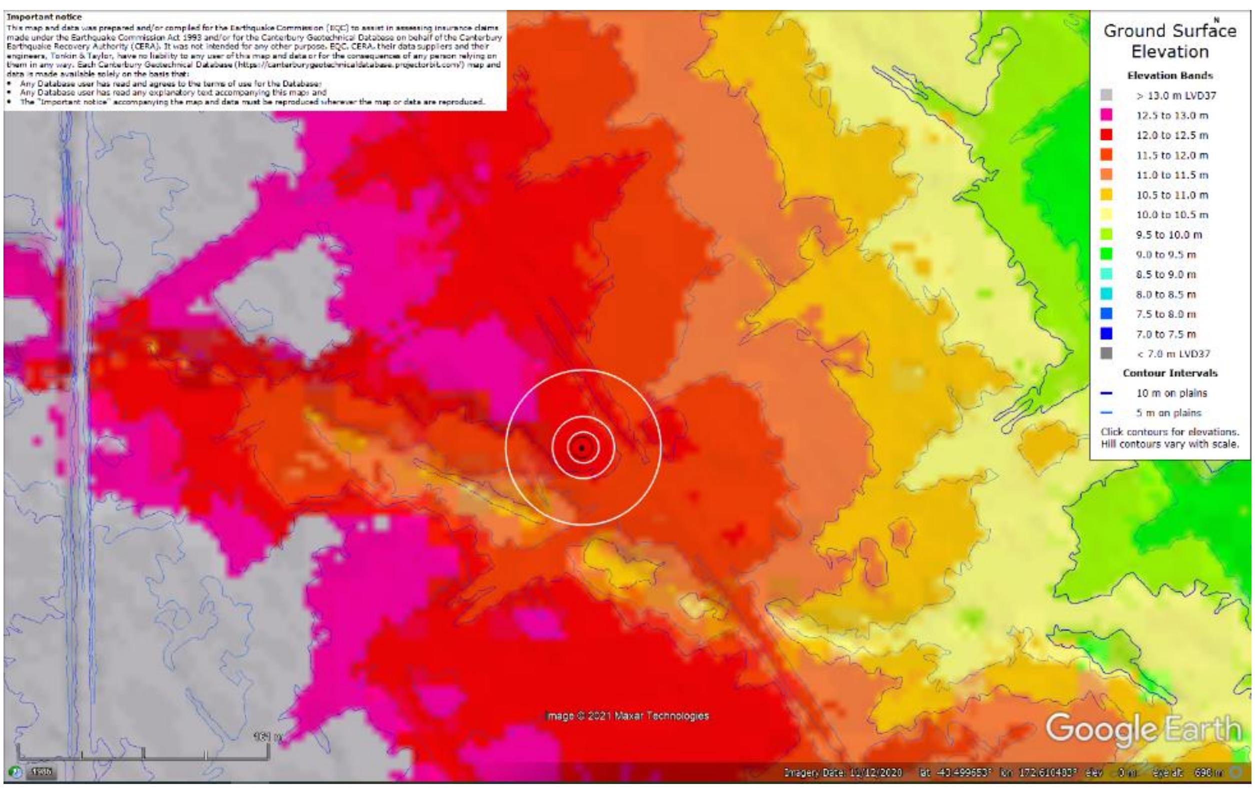

Figure 43: Ground surface elevation according to the Sep-11 LiDAR survey.

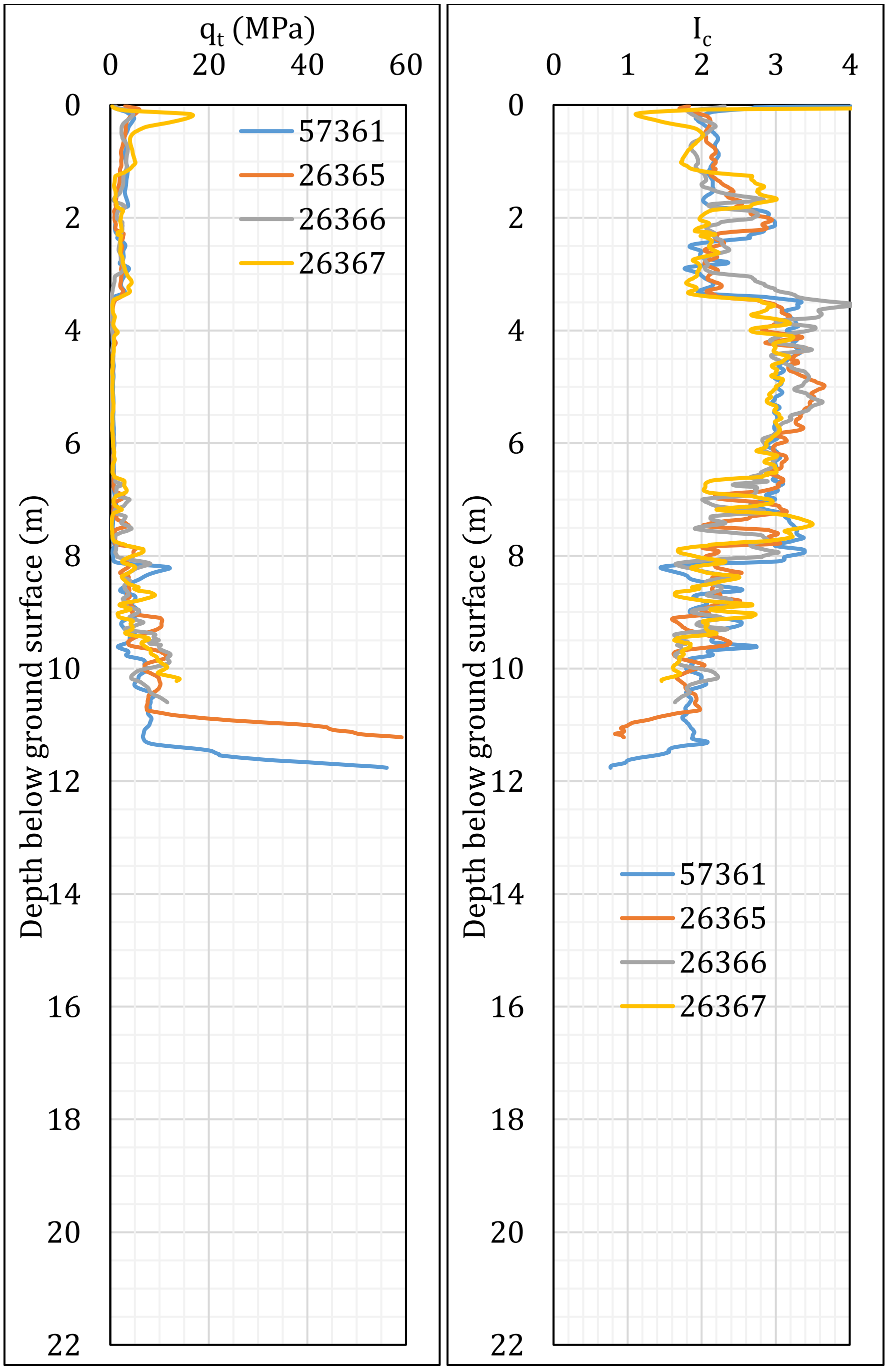

Figure 44: q_t and I_c profiles.

Note 4: The selection of CPTs for the area considered for settlement assessment (Figure 1) is based on the proximity of the CPTs to the considered areas. In accordance with that, the following table shows CPTs that were used for the volumetric settlement analysis in *Cliq v.3.0.3.2*, a CPT soil liquefaction software developed by GeoLogismiki. (The average volumetric settlements were reported in Table 8.)

Table 5: CPT profiles used in volumetric settlement analysis for areas selected for settlement assessment.

CPT ID No.	10-m buffer	20-m buffer	50-m buffer
57361 (56739)	✓	✓	✓
26365 (27455)		✓	✓
26366 (27456)			✓
26367 (27457)			✓

Note: It is assumed that the volumetric settlement below the 12-m depth is negligible.

Table 6: CPT-based results.

		CPT ID			
EQ Event	Parameter	57361	26365	26366	26367
Sep-10	S_{V1D} (mm)	82	83	82	91
	LSN	14	19	16	19
	LPI	5	5	5	6
	LPI_{ish}	2	2	2	3
	$D_{FS<1}$ (m)	2.42	1.60	2.16	1.94
Feb-11	S_{V1D} (mm)	93	99	95	102
	LSN	17	26	22	24
	LPI	7	8	8	9
	LPI_{ish}	4	4	4	6
	$D_{FS<1}$ (m)	2.38	1.24	1.40	1.82
Jun-11	S_{V1D} (mm)	18	17	22	28
	LSN	3	4	4	5
	LPI	0	0	0	0
	LPI_{ish}	0	0	0	0
	$D_{FS<1}$ (m)	undet.	undet.	undet.	undet.
Dec-11	S_{V1D} (mm)	30	30	37	45
	LSN	5	7	6	8
	LPI	0	1	1	1
	LPI_{ish}	0	0	1	1
	$D_{FS<1}$ (m)	9.14	undet.	7.26	6.62

Notes: $D_{FS<1}$ = Depth to the first liquefiable layer (FS_L<1) that is at least 200-mm thick, as determined by the Boulanger and Idriss (2016) liquefaction-triggering procedure (P_L=50%, C_{FC}=0.13, and $I_{c,cutoff}$ =2.6), and exported from *Cliq v.3.0.3.2*; undet. = the specified soil layer was not detected; The S_{V1D}, LSN, and LPI values are computed for a depth range from 12 m to 20 m.

Note 5: Based on the borehole log (BH 57238, Figure 1), the groundwater table is at a depth of 2.6 m below the ground surface. The soil profile consists of (1) organic silt, OL, topsoil to a depth of 0.15 m, (2) fine sand, SP, to a depth of 1.75 m, (3) silt, ML, to a depth of 2.5 m, (4) fine sand, SP, to a depth of 3.3 m, (4) silt, ML, to a depth of 3.95 m, (5) peat, Pt, to a depth of 4.25 m, (6) silt, ML, to a depth of 9.1 m, (7) silty fine sand, SM, to a depth of 9.4 m, (8) silt, ML, to a depth of 9.6 m, (9) fine sand, SP, to a depth of 12.0 m, (10) sandy fine to coarse gravel, GW, to a depth of 14.75 m, (11) silt, ML, to a depth of 15.0 m, and (12) fine to medium sand, SP, to a depth of 15.65 m (the end of the borehole). All soil layers (except the topsoil) are the Yaldhurst members of the Springston formation.